Applied Surface Science xxx (2015) xxx–xxx

Contents lists available at ScienceDirect

Applied Surface Science

journal homepage: www.elsevier.com/locate/apsusc

Laser-assisted synthesis of ultra-small anatase TiO_2 nanoparticles

M. Amin [a], J. Tomko [b], J.J. Naddeo [b], R. Jimenez [b], D.M. Bubb [b], M. Steiner [c], J. Fitz-Gerald [c], S.M. O'Malley [b,*]

[a] Department of Physics, University of Maryland, College Park, MD 20742, USA
[b] Department of Physics, Rutgers University, Camden, NJ 08102, USA
[c] Department of Materials Science & Engineering, University of Virginia, Charlottesville, VA 22904, USA

ARTICLE INFO

Article history:
Received 4 October 2014
Received in revised form
30 December 2014
Accepted 30 December 2014
Available online xxx

Keywords:
Laser synthesis
Titanium dioxide nanoparticles
Fragmentation
Shockwave propagation
Photocatalysis

ABSTRACT

Titanium dioxide is one of the most important materials today in terms of green technology. In this work, we synthesis ultra-small titanium dioxide nanoparticles (NPs) via a two step process involving infrared laser ablation of a bulk titanium target in DDI water and subsequent irradiation of the colloidal solution with visible light. The as-prepared NPs contain defect states related to oxygen vacancies which lead to visible light sensitization as observed by photodegradation of methylene blue. Irradiation of the colloidal TiO_2 solution, with a 532 nm picosecond laser, lead to fragmentation and ultimate formation of ultra-small (<3 nm) anatase particles. Shadowgraph was utilized to capture shockwave and cavitation bubble propagation during both the ablation and fragmentation processes. High-frequency ripples within the primary shockwave are identified as coming from laser induced stress-wave reflections within the metal target. A blueshift of the bandgap, for the ultra-small NPs, is explained by quantum confinement effects and rationalized using the Brus model.

1. Introduction

Titanium dioxide has long been known as a promising material for applications such as a photocatalyst in decomposition of pollutants, as a photo-voltaic for green energy solar technology, and as a bactericidal agent, especially due to its biocompatibility. One challenge in utilizing TiO_2 in these applications is that it has a wide bandgap and thus requires UV-light to initiate direct photo-excitation.

In nanoparticle form, one of TiO_2's most important characteristics is that it can generate reactive oxygen species (ROS). The applicability of TiO_2 would be greatly enhanced if its photo-activity was extended into the visible region of the spectrum. Various materials can be used as sensitizers (e.g. Ag NPs, graphene), however, the strength of the photo-catalytic response of the TiO_2 quickly destroys the sensitizers. Therefore such measures are invariably stop-gap and temporary. Alternatively, intermediate gap states can be introduced via defects, such as oxygen vacancies [1]. Titanium dioxide is also polymorphic and can be synthesized in the rutile, brookite, or anatase crystalline phases, allowing for the creation of a wide number of phases and nanostructures.

Laser ablation in liquids (LAL) [2,3] is a promising technique for the creation of suspensions of nanoparticles and nanocomposites. It is a reliable method to produce precursor-free colloidal solutions. While it is most typically used for metals and semiconductors [4,5], it can also be used for organic materials as well [6].

It is well known that anatase TiO_2 displays a higher photocatalytic efficiency than the rutile phase [7,8]. There is also strong evidence that surface hydroxylation and oxygen vacancies act as charge carrier trapping sites, thus reducing recombination and enhancing the photo-activity of the NPs [9,10]. Additionally, the smaller the particle size the less distance photogenerated charge carriers have to travel to reach surface reaction sites [11]. Therefore, we have focused on the production of suspensions of anatase nanoparticles of very small size (<3 nm) in this work and we have explored their effectiveness in the photocatalytic degradation of the dye, methylene blue.

2. Results

2.1. Experimental conditions

The initial colloidal suspensions were produced using a picosecond Nd:YAG laser (Ekspla PL2241, 25 ps) operating at its fundamental wavelength (1064 nm) and a repetition rate of 250 Hz. A Ti plate was placed in a 50 mL beaker on top of a short

* Corresponding author. Tel.: +1 8562256159.
E-mail address: omallese@camden.rutgers.edu (S.M. O'Malley).

http://dx.doi.org/10.1016/j.apsusc.2014.12.191
0169-4332/

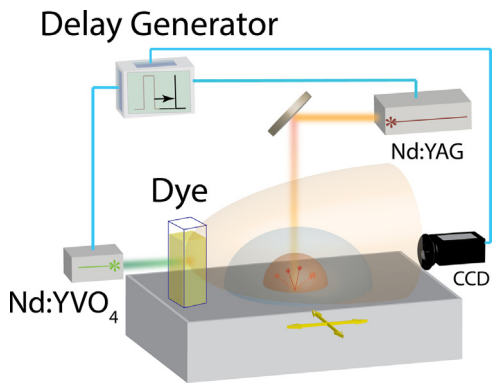

Fig. 1. Schematic of the imaging apparatus. The setup contained a 25 ps Nd:YAG (1064 nm) laser for ablation of the titanium plate submerged in an optical cell. The ablation process was back illuminated using a fluorescent dye contained in a cuvette and excited by a Nd:YVO_4 (532 nm) laser. A digital delay generator controlled timing between the Nd:YAG laser, the Nd:YVO_4 laser, and the CCD camera's shutter. *Note*. The optical cell was omitted in the illustration for clarity.

stainless steel platform, which allowed for a magnetic stirrer to be placed underneath the target; the liquid height above the target was 15 mm. Fluence at the target surface was 490 mJ/cm^2. The approximately square plate, with an area of ~4.0 cm^2, was moved by a motorized *XY* translation stage in order to uniformly ablate the sample. Ablation took place for 8 min and a turbid solution with a blue hue developed.

For shadowgraph imaging of the shockwave/cavitation bubble, the titanium target was placed into a rectangular (type 96) spectrophotometer cell with polished front and back surfaces. Images were taken using a Sentech STC-TB202USH-ASH CCD camera equipped with a macro lens. A 532 nm Nd:YVO_4 laser (Ekspla NL-201, 10 ns) incident upon a cuvette of Rhodamine dye served as the camera's flash. The timing between laser pulses was controlled by a four-channel digital delay generator (Berkeley Nucleonics Corporation 575), and the total optical jitter was determined to be ~20 ns. Note that the camera's shutter is opened before the ablation pulse arrives. A schematic of the process, along with the imaging apparatus is shown in Fig. 1.

2.2. Particle synthesis, post-irradiation, and characterization

The absorbance spectrum shows a broad peak that extends well into the near-IR as shown in Fig. 2. Dynamic light scattering (DLS) measurements show a wide distribution of particle sizes with a mean hydrodynamic diameter of 132 ± 55 nm. HR-TEM images agree well with the DLS measurements and reveal the NPs to be polymorphic, predominantly consisting of rutile and amorphous phases with a small admixture of anatase. In the size histogram, two distinct peaks are present at 100 ± 40 nm and 225 ± 25 nm. Additionally, some hollow nanospheres are present [12]. The large absorption tail that persists into the near-IR is indicative of mid-gap defect states [10], so the as-synthesized NPs are best described by the chemical formula TiO_x where x is between 1 and 2.

Further examination of the HR-TEM images reveals that the smaller particles are crystalline and anatase. The particle in the left frame of Fig. 3 clearly shows spacing associated with the {0 0 5} plane family. Indexing of the particle in the right frame reveals a lattice spacing of about 2.3 Å, which is consistent with the {0 2 0} rutile family of planes.

2.2.1. Post-irradiation

Pulsed laser irradiation of colloidal NP solutions has been shown to induce size reduction and homogenization, shape evolution, structural transformations, and compositional changes of the NPs [13–17]. The incident radiation absorbed by the NPs may come about through either excitation of interband transitions or excitement of SPR modes within the metal NPs. In the case of ultrashort laser pulses, multi-photon absorption can also occur. The current belief is that the NPs may experience either melting, thermal evaporation [18,19], or Coulomb explosion where strong repulsive forces between similarly charged regions within a particle cause it to fragment [17,20]. The fragmentation mechanism experienced by the NPs during irradiation depends on several factors, some intrinsic to the particle (e.g. melting point, and absorption coefficient) while others are related to the laser source (e.g. pulse duration, and wavelength). In the case of short (<30 ps) lasers pulses and high intensities it is possible to have direct photoionization of the particles that leads to Coulomb explosion.

The UV–vis spectrum displayed in Fig. 2 is indicative of particles with a high defect density, most likely oxygen vacancies. The initial bandgap extracted from a Tauc plot is of the order of 0.7 eV. The spectra was fitted to a Tauc plot [21] for indirect transitions with $(h\nu\alpha)^{(1/2)} = A(h\nu - E_g)$ where $h\nu$ is the photon energy, α is the extinction coefficient as determined from the Beer–Lambert law, A is a proportionality constant, and E_g is the band gap.

After synthesis, the particles were irradiated with a 25 ps 532 nm laser, resulting in a significant size reduction along with changes to the UV-vis spectrum. A 35 mm focal length plano convex lens was used to bring the 0.66 mJ laser pulses to a beam waist of about 3 μm. HR-TEM gives an average hydrodynamic diameter of 2.17 ± 0.59 nm after 20 min of irradiation in agreement with

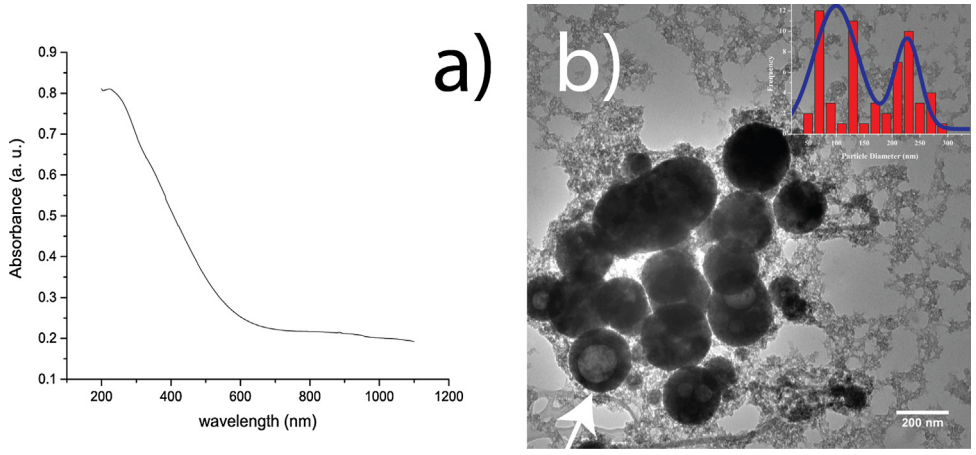

Fig. 2. (a) UV–vis spectrum of as-synthesized TiO_x nanoparticles and (b) HR-TEM of the resulting particles with histogram in the inset.

Please cite this article in press as: M. Amin, et al., Laser-assisted synthesis of ultra-small anatase TiO_2 nanoparticles, Appl. Surf. Sci. (2015), http://dx.doi.org/10.1016/j.apsusc.2014.12.191